Control of high-order harmonic generation with two-colour laser field*

Dai Jun(戴 君), Zeng Zhi-Nan(曾志男)†, Li Ru-Xin(李儒新), and Xu Zhi-Zhan(徐至展)

State Key Laboratory of High Field Laser Physics, Shanghai Institute of Optics and Fine Mechanics, Chinese Academy of Sciences, Shanghai 201800, *China*

(Received 3 March 2010; revised manuscript received 22 May 2010)

We numerically investigate the high-order harmonic generation with two-colour optical field, taking into consideration the propagation effects. Some harmonics can be dramatically enhanced at a certain delay between the fundamental pulse and its second harmonics. Choice of the enhanced harmonics can be realised by changing the time delay between the two laser pulses.

Keywords: high-order harmonic, two-colour laser field, Lewenstein model
PACC: 3280, 4250, 7220H

1. Introduction

High-order harmonic generation (HHG) from the atomic gases has been intensively investigated in the past two decades.[1−5] More recently, HHG has become substantially important for a wide range of diverse applications. Particularly, it has successfully opened a new route to attosecond (as) science.[6−8] It can also produce coherent soft x-ray radiation in the important spectral region, such as the 'water window'.[9,10]

To make the HHG more useful, a lot of effort has been devoted to improving its energy. To generate the harmonics efficiently, it is important to achieve a perfect phase matching between the driving laser pulse and the generated harmonic field.[11] But, many effects, e.g. dispersion, plasma, etc, will destroy the phase matching process. Although these conditions can be controlled to make the constructively interference, the phase matching can only be realised in a narrow spectral bandwidth. In our work, we theoretically investigate the macroscopic effects of the harmonic generation by two-colour field, with which HHG efficiency can be readily controlled.

2. Model and method

The simulation is employed by properly taking into account both the single-atom (microscopic) response to the laser pulse and the propagation (macroscopic) effect. The microscopic model presented here is based on an extension of the Lewenstein model[1] and the nonlinear dipole momentum is (in atomic units (a.u.))

$$\tilde{d}_{\rm h}(\tau) = \sum_{\tau_{\rm b}} \tfrac{1}{\sqrt{i}} a_{\rm ion}(\tau_{\rm b}) \tilde{a}_{\rm pr}(\tau_{\rm b}, \tau) a_{\rm rec}(\tau). \qquad (1)$$

The tilde here denotes complex quantities. Three probability amplitudes in Eq. (1) given by Eqs. (35)–(39) in Ref. [12] in detail, can be interpreted in terms of the semiclassical three-step model of HHG:[13] the electron first tunnels through the potential barrier with a ratio $a_{\rm ion}$ at an instant $\tau_{\rm b}$, then propagates in the laser field described by $\tilde{a}_{\rm pr}$, and finally recombines with the parent ions with a probability $a_{\rm rec}$ to emit high-energy photons.

For the collective response of the atoms, the propagation of the driving laser and the high harmonic fields are solved with the following equations,[14] respectively,

$$\partial_\xi E_{\rm l}(\xi,\tau) - \hat{D} E_{\rm l}(\xi,\tau') = -\frac{1}{2c}\int_{-\infty}^{\tau} \omega_{\rm p}^2(\xi,\tau') E_{\rm l}(\xi,\tau'){\rm d}\tau' - \frac{W_{\rm b}}{2\varepsilon_0 c}\frac{\partial_\tau n_{\rm e}(\xi,\tau)}{E_{\rm l}(\xi,\tau)} - \frac{\zeta^{(1)}}{c}\partial_\tau[1-n_{\rm e}(\xi,\tau)]E_{\rm l}(\xi,\tau), \quad (2)$$

$$(\partial_\xi + \alpha_{\rm h}) E_{\rm h}(\xi,\tau) = \frac{-1}{2\varepsilon_0 c}\partial_\tau \tilde{P}_{\rm h}[E_{\rm l}(\xi,\tau)] + {\rm c.c.}, \qquad (3)$$

*Project supported by Chinese Academy of Sciences, the National Natural Science Foundation (Grant Nos. 10734080, 10523003, 60921004, 10904157, and 60978012), 973 Project (Grant No. 2006CB806000), and Shanghai Commission of Science and Technology (Grant Nos. 06DZ22015 and 07PJ14091).

†Corresponding author. E-mail: zhinan_zeng@mail.siom.ac.cn

© 2010 Chinese Physical Society and IOP Publishing Ltd

where $E_{\rm l}$ and $E_{\rm h}$ are the laser field and high harmonics, respectively. Here, we change to the moving coordinate frame in vacuum, $\tau = t - z/c$ same as Eq. (1) and $\xi = z$. The operator $\hat{D} = (c/2)\nabla_{\perp}^2 \int_{-\infty}^{t} {\rm d}t'$ stands for the diffraction of the driving laser pulse, while the diffraction of the harmonic pulse is negligible. The free electron density can be written as

$$n_{\rm e}(\xi,\tau) = n_{\rm a}\left(1 - \exp\left[-\int_{-\infty}^{t} {\rm d}\tau' w\left\{E_{\rm l}(\xi,\tau')\right\}\right]\right), \tag{4}$$

where $n_{\rm a}$ is the density of atoms, $w(E_{\rm l})$ is the optical field ionization rate. The plasma frequency is determined by

$$\omega_{\rm p} = \sqrt{\frac{e^2 n_{\rm e}(\xi,\tau)}{m\varepsilon_0}}. \tag{5}$$

First, a Gaussian beam is assumed as the initial condition to evolve Eq. (2), which is given in the next section, and the dipole moment $\tilde{d}_{\rm h}$ is obtained by calculating the single-atom response via Eq. (1). The parameter c, e, m, ε_0, $W_{\rm b}$, $\alpha_{\rm h}$ and $\zeta^{(1)}$ refer to the vacuum light velocity, electron charge, electron mass, permittivity of free space, atomic ionisation potential, XUV absorption coefficient, and linear susceptibility of neutral atoms, respectively.

3. Result and discussion

In this simulation, the initial two-colour field can be written as

$$\begin{aligned} E_{\rm l} &= E_1 + E_2 \\ &= \tilde{A}_1 \exp\left\{-{\rm i}\left[\frac{\omega_0 z_1(\tau-\tau_0)}{c} - \arctan\left(\frac{2cz_1(\tau-\tau_0)}{\omega_0 a_1^2}\right)\right]\right\} {\rm sech}\left[2\ln(1+\sqrt{2})(\tau-\tau_0)/\tau_{p_1}\right] \\ &\quad + \tilde{A}_2 \exp\left\{-{\rm i}\left[\frac{2\omega_0 z_2(\tau)}{c} - \arctan\left(\frac{2cz_2(\tau)}{2\omega_0 a_2^2}\right)\right]\right\} {\rm sech}\left[2\ln(1+\sqrt{2})\tau/\tau_{p_2}\right], \end{aligned} \tag{6}$$

where $\tilde{A}_1$ and $\tilde{A}_2$ are the complex amplitudes of the electric fields of the fundamental and the second harmonics, respectively; ω_0 is the central frequency of the fundamental pulse; a_1 and a_2 are the beam waist of the fundamental and the second harmonics pulses, respectively; τ_{p_1} and τ_{p_2} denote the corresponding FWHM(full width at half maximum) pulse durations. In Eq. (6) τ_0 is the relative time delay between the two-colour fields, creating a phase shift of $2\pi\tau_0/{\rm T}$, where T is the optical period of the fundamental laser pulse. Figure 1 shows the electric field of the two-colour pulses on the axis, where the wavelength $\lambda_{1,2} = 800$ nm/400 nm, the peak electric field intensity $I_{1,2} = 2.0 \times 10^{14}$ W/cm^2/0.2×10^{14} W/cm^2, the FWHM pulse durations $\tau_{p_{1,2}} = 40$ fs/40 fs, the beam waist $a_{1,2} = 40$ μm/40 μm. We choose the propagation length to be 1.8 mm, and the time delay τ_0 0, 416.7, 833.3 and 1250.0 as.

Figure 2 represents the HH spectra generated by the four driving pulses shown in Fig. 1 with and without considering propagation effects. In the figure, only the HH spectra on the axis are considered. According to Fig. 2(a), we can see that the maximal difference of HH amplitude generated from the two colour laser pulses with various time delays is about 1.08×10^{-10} a.u. in these four chosen orders (28, 29, 30, 31), whereas, which is about 2.52×10^{-4} a.u. after propagation shown in Fig.2.(b). After propagation, the HHG peaks in Fig. 2(b) can be more clear.

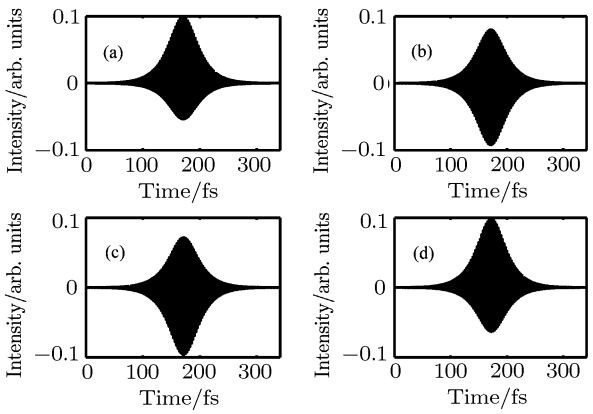


Fig. 1. Electric fields of the two-colour pulses without time delay (a), and with a time delay 416.7 as (b), 833.3 as (c), and 1250.0 as (d).

To study the propagation effects of the HHG process, we represent the intensity of the 27th harmonic evolving in the 1.8 mm propagation length in Fig. 3.

To make the simulation result close to the reality, the atom density distribution with Gaussian profile upon the propagation length is adopted in this simulation, in which the corresponding FWHM of the density distribution is 1 mm, shown in Fig. 3.

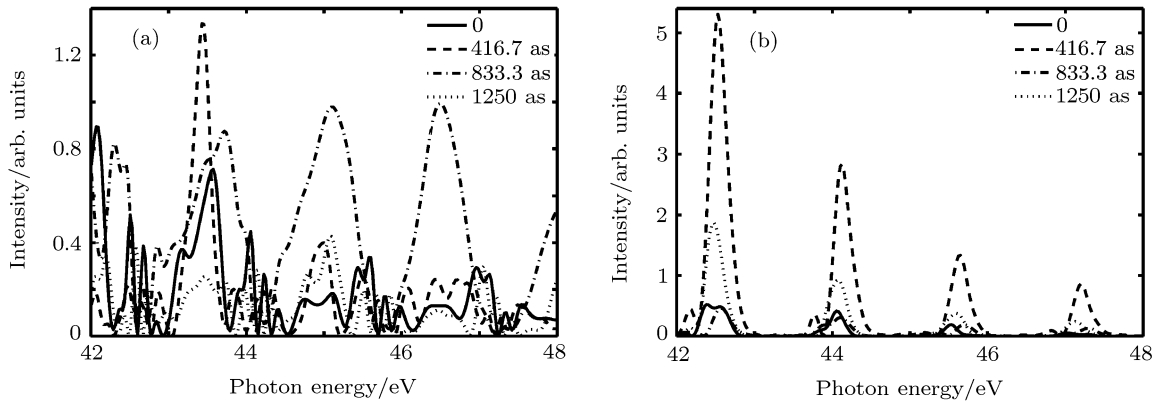


Fig. 2. Harmonic spectra before propagation (a) and after propagation (b), obtained by the two colour driving laser pulses with different time delays 0 (solid line), 416.7 as (dashed line), 833.3 as (dot-dashed line) and 1250.0 as (dotted line), respectively.

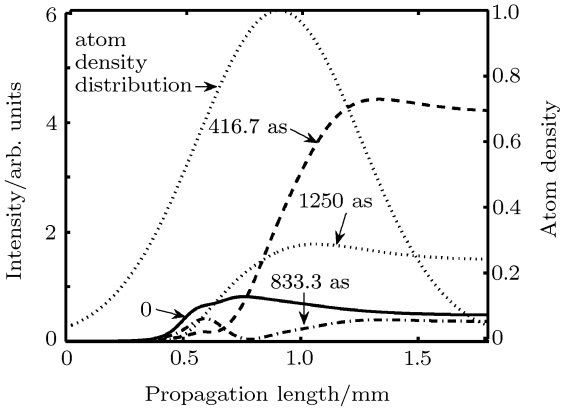


Fig. 3. Evolution of the 27th harmonic upon propagation of the two-colour laser field with different time delays: 0 (solid line), 416.7 as (dashed line), 833.3 as (dot-dashed line) and 1250 as (dotted line). The atom density distribution (dashed line) is also added in the figure, in which the corresponding FWHM is 1 mm.

As well known, in an ideal case, the amplitude of harmonics can be enhanced substantially due to the constructive interference resulting from the phase matching between the driving laser pulse and the high-order harmonics. In the practical scenario, a full description of HHG should consider the negative effect for the destructive interference in the propagation process, including mainly the absorption losses and free-electron-induced dephasing, setting a limit to the maximum achievable harmonic yield. We can make an analysis from Fig. 3 that, as the propagation distance increases gradually, the negative effect imposed on HHG becomes more and more severe, arising from more free electrons and more absorption losses. Consequently, the 27th harmonic produced by the two-colour pulses with different time delays, is suppressed to different degrees when the propagation distance exceeds 0.6 mm. Note that the harmonic intensity(dashed line) corresponding to the time delay 416.7 as between the two-colour fields can be enhanced to 4.221×10^{-4} a.u. after propagation, about one order of magnitude higher than the minimum. It is indicated that the collective effect of the atoms can be controlled via varying the time delay between the two-colour driving laser pulses.

We also investigate the effect of driving laser intensity ratio $E02/E01$ ($E01$ and $E02$ represent the intensities of the fundamental and the second harmonic pulse, respectively) in HHG. We change the intensity ratio $E02/E01$ from 0.05 to 0.15 with the intensity of the fundamental laser pulse unchanged as 2.0×10^{14} W/cm^2. Other parameters in the calculation are the same as those for Fig. 2. Figure 4 depicts the intensity distribution of HH with respect to harmonic order chosen from 11 to 39 (x-axis) and time delay (y-axis), with three different intensity ratios at the beginning and the end of the propagation. As shown in Fig. 4, via propagation through gas medium, we can make the harmonic intensity converge to some higher orders of harmonics ranging from 23 to 29, as in Fig. 4(d), by adjusting the relative intensities between the fundamental and frequency-doubled fields. With the increase in intensity ratio E_{02}/E_{01}, the harmonic intensity distribution tends to extend to lower orders, although the profile of the distribution is similar to Fig. 4(d). The maximum harmonic intensities against the ratio of relative intensities are listed in Table 1. As shown in Table 1, the maximum harmonic intensity appearing at the intensity ratio $E_{02}/E_{01} = 0.05$ is higher by $\sim$ 42.6% and $\sim$ 93.8% than those obtained at $E_{02}/E_{01} = 0.1$, 0.15. When $E_{02}/E_{01} = 0$, the two colour driving pulse is just a single long pulse, for which the maximum harmonic in-

tensity is 6.288×10^{-4} a.u., smaller than that obtained at $E_{02}/E_{01} = 0.05$. This means that there is an optimum value for E_{02}/E_{01} around 0.05 to obtain the maximum HH intensity.

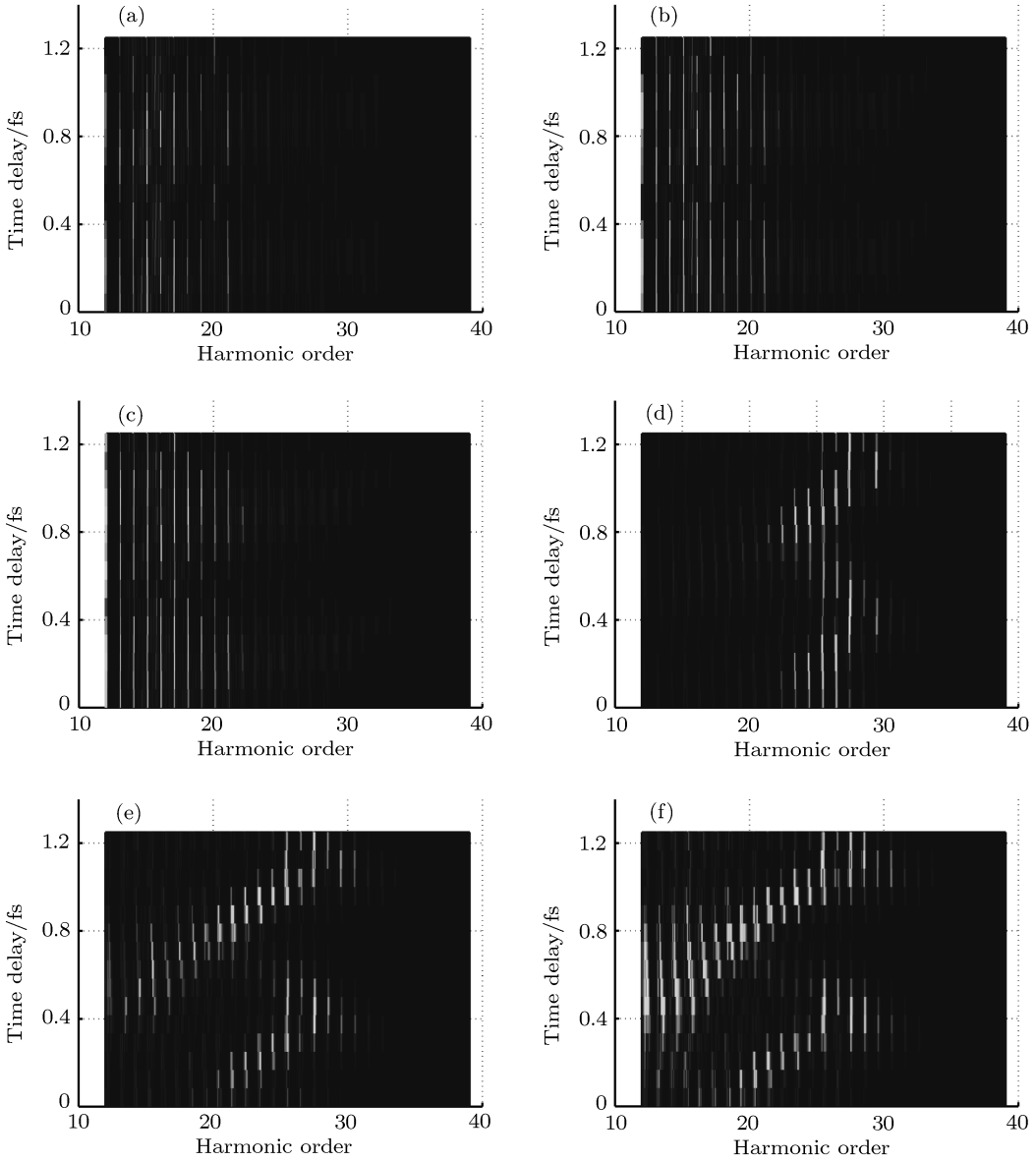


Fig. 4. Harmonic intensity distribution versus harmonic order and time delay with different intensity ratio of the two-colour driving pulses, $E_{02}/E_{01} = 0.05$ (a) and (d), 0.1(b) and (e), 0.15(c) and (f), before and after propagation. Figures (a), (b), (c) on the left side show the HHGs before propagation, the rest denote those after propagation.

Table 1. Maximum harmonic intensity versus the relative intensity between the two-colour fields.

E_{02}/E_{01}	0	0.05	0.1	0.15
$E_{\rm hmax}$ (a.u. $\times10^{-4}$)	6.288	11.24	7.879	5.799

To investigate the propagation effects on the higher harmonics generation, especially the 'water window' region, a 30 fs/2000 nm and a frequency-doubled 30 fs/1000 nm pulses are combined to serve as the driving pulse for generating harmonics. The intensities of the fundamental and the second harmonic pulses are 4.0×10^{14} W/cm^2 and 0.4×10^{14} W/cm^2, respectively. The propagation length is 1.8 mm, the

same value as mentioned above. Figure 5 shows the harmonics generated by the two-colour pulses with time delays 1041.7 as, 2083.3 as and 3125.0 as, respectively, at the end of propagation. From the figure we can see, the intensity of the HHG can be changed by two orders of magnitude, which means that the two-colour laser field can also be used to control the phase matching of the HHG in the water window.

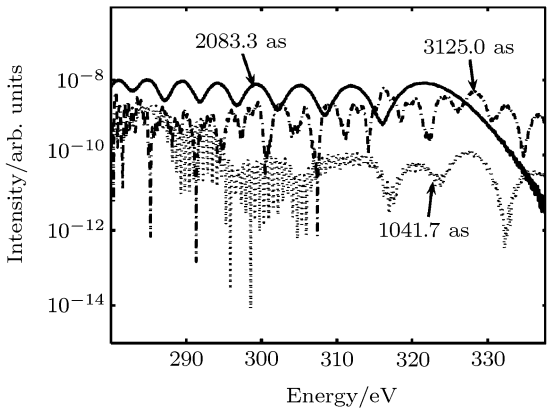


Fig. 5. Harmonics generated by two-colour laser pulses (2000 nm/1000 nm) with different time delays 1041.7 as (dotted line), 2083.3 as (solid line) and 3125.0 as (dot-dashed line), respectively.

4. Summary

In this paper, we theoretically investigated high-order harmonic generation in two-colour laser fields by considering macroscopic effects. The results show that HHG is sensitive to the relative phase and intensity ratio of the two-colour laser fields. Consequently, by adjusting the time delay and the relative intensity between the fundamental and frequency-doubled laser pulses, a specific range of harmonics can be enhanced dramatically. In 'water window' region, the variation of HH intensity with time delay can even reach by 2 orders of magnitude. The results indicate that the two-colour field is a powerful tool to control the frequency of the enhanced HHG.

References

[1] Lewenstein M, Balcou P, lvanov M Y, L'Huillier A and Corkum P B 1994 *Phys. Rev.* A **49** 2117
[2] Agostini P and DiMauro L 2004 *Rep. Prog. Phys.* **67** 813
[3] Durfee C G, Rundquist A R, Backus S, Herne C, Murnane M M and Kapteyn H C 1999 *Phys. Rev. Lett.* **83** 2187
[4] Zhang X S, Lytle A L, Popmintchev T, Zhou X, Kapteyn H C, Murnane M M and Cohen O 2007 *Nat. Phys.* **3** 270
[5] Tamaki Y, Itatani J, Nagata Y, Obara M and Midorikawa K 1999 *Phys. Rev. Lett.* **82** 1422
[6] Hentschel M, Kienberger R, Spielmann Ch, Reider G A, Milosevic N, Brabec T, Corkum P, Heinzmann U, Drescher M and Krausz F 2001 *Nature* **414** 509
[7] Gohel C, Udem T, Herrmann M, Rauschenberger J, Holzwarth R, Schuessler H A, Krausz F and Hänsch T W 2005 *Nature* **436** 234
[8] Mairesse Y, de Bohan A, Frasinski L J, Merdji H, Dinu L C, Monchicourt P, Breger P, Kovacev M, Taïeb R, Carré B, Muller H G, Agostini P and Salières P 2003 *Science* **302** 1540
[9] Spielmann Ch, Burnett N, Sartania S, Koppitsch R, Schnurer M, Kan C, Lenzner M, Wobrauschek P and Krausz F 1997 *Science* **278** 661
[10] Chang Z, Rundquist A, Wang H, Murnane M M and Kapteyn H C 1997 *Phys. Rev. Lett.* **79** 2967
[11] Meyer S, Chichkov B N, Wellegehausen B and Sanpera A 2000 *Phys. Rev.* A **61** 063811
[12] Brabec T and Krausz F 2000 *Rev. Mod. Phys.* **72** 545
[13] Corkum P B 1993 *Phys. Rev. Lett.* **71** 1994
[14] Milosevic N, Scrinzi A and Brabec T 2002 *Phys. Rev. Lett.* **88** 093905